Table III. Selected Bond Distances (Å) and Angles (deg) for Ph$_2$Bi–SePh

Bi–Se	2.704 (3)	Bi–C(1)	2.25 (1)
Se–C(13)	1.92 (1)	Bi–C(7)	2.25 (1)
Se–Bi–C(1)	97.4 (3)	Bi–C(7)–C(8)	120.4 (9)
Se–Bi–C(7)	87.4 (3)	Bi–C(7)–C(12)	119.5 (10)
C(1)–Bi–C(7)	90.8 (4)	Bi–Se–C(13)	100.0 (4)
Bi–C(1)–C(2)	114.8 (9)	Se–C(13)–C(14)	118.3 (9)
Bi–C(1)–C(6)	124.7 (9)	Se–C(13)–C(18)	121.6 (8)

nucleophilic attack at the *metal*. On the other hand, insertion of carbene from CH_2N_2 into the tellurium–tellurium bond of Te$_2$Ph$_2$[22] has been found to occur at room temperature, whereas the insertion into Se–Se and S–S bonds required the use of visible light.

We have recently reported the oxidation of Bi$_2$Ph$_4$ by several reagents such as O$_2$, S$_8$, *p*-benzoquinone, and I$_2$.[3] Elemental selenium gives the product resulting from the oxidative insertion into the Bi–Bi bond (see eq 5). No reaction was found to occur

$$Bi_2Ph_4 + (1/n)Se_n \rightarrow Ph_2Bi–Se–BiPh_2 \qquad (5)$$
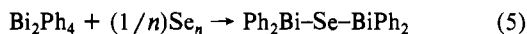
with elemental tellurium, although this may be due simply to difficulties connected with the heterogeneus nature of the system.

While this work was in progress, similar results were found for Bi$_2$(*p*-C$_6$H$_4$Me)$_4$, which is also unreactive toward tellurium.[15b]

Structure Study. The crystal of Ph$_2$BiSePh, obtained by slow crystallization at about +5 °C, belongs to the enantiomeric space group *P*2$_1$2$_1$2$_1$. This is a quite common case of enantiomeric enrichment during crystallization.[23]

All intermolecular contacts in the structure conform to normal van der Waals interactions; the shortest contact is C(6)⋯C(8) ($^3/_2$ − *x*, −*y*, $^1/_2$ + *z*), i.e. 3.48 (2) Å.

The molecular unit of Ph$_2$Bi–SePh is illustrated by the ORTEP drawing of Figure 1, which also gives the adopted numbering scheme. The coordination geometry about the bismuth atom can be described as pyramidal with the metal displaced 1.327 Å from the plane defined by Se, C(1), and C(7). The bond angles around bismuth are all significantly less than the tetrahedral value, thus indicating that the lone pair has considerable s character. In this respect, the geometry around bismuth is virtually identical with those observed in Bi$_2$Ph$_4$[3] and in [Co(BiPh$_2$)(CO)$_3$(PPh$_3$)].[24] The

two Bi–C bond distances, both of 2.25 (1) Å (see Table III), are practically the same as they are in the two aforementioned compounds, in which these values are 2.28 (2), 2.26 (2) and 2.25 (2), 2.28 (2) Å, respectively. The Bi–Se bond distance of 2.704 (3) Å compares fairly well with the 2.684 Å reported for BaBiSe$_3$[25] and is slightly shorter than the strongest bonds (2.82–2.85 Å) in Bi$_2$Se$_3$.[26] However, if we consider the Bi–Bi distance in Bi$_2$Ph$_4$[3] (2.990 (2) Å) and the Se–Se distance in Se$_2$Ph$_2$[27] (2.29 (1) Å), we come to the conclusion that the observed Se–Bi distance of 2.704 (3) Å is somewhat longer than expected (2.64 (1) Å) on the basis of the distance in the homonuclear species.

The Bi–Se bond makes angles of 46.4 (3), 44.1 (3), and 16.6 (2)° with the normals to the C(1)⋯C(6), C(7)⋯C(12), and C-(13)⋯C(18) planes, respectively.

The Se–C bond distance was found to be 1.92 (1) Å, which is very similar to the values previously observed for this bond (e.g. 1.93 (5) Å in Se$_2$Ph$_2$,[27] 1.92 (4) Å in di-*p*-tolyl selenide,[28] 1.936 (9), 1.960 (12), and 1.962 (12) Å in η^7-C$_7$H$_7$Mo(μ-SePh)$_3$Mo-(CO)$_3$,[29] and 1.92 (2) Å in Mn$_2$Br$_2$(CO)$_6$Se$_2$Ph$_2$[30]). The angle at Se is 100.0 (4)°, and the displacement of this atom from the plane through the attached phenyl ring is 0.09 Å.

(22) Petragnani, N.; Schill, G. *Chem. Ber.* **1970**, *103*, 2271.
(23) Collet, A.; Brienne, M. J.; Jacques, J. *Chem. Rev.* **1980**, *80*, 215.
(24) Calderazzo, F.; Poli, R.; Pelizzi, G. *J. Chem. Soc., Dalton Trans.* **1984**, 2535.

(25) Volk, K.; Cordier, G.; Cook, R. *Z. Naturforsch, B: Anorg. Chem., Org. Chem.* **1980**, *35B*, 136. Quoted from: Brown, I. D.; Brown, M. C.; Hawthorne, F. C. BIDICS, Institute for Materials Research, McMaster University, Hamilton, Ontario, Canada, 1981.
(26) Atabaeva, E. Ya.; Mashkov, S. A.; Popova, S. V. *Kristallografiya* **1973**, *18*, 173; *Chem. Abstr.* **1973**, *78*, 116444n.
(27) Marsh, R. E. *Acta Crystallogr.* **1952**, *5*, 458.
(28) Blackmore, W. R.; Abrahams, S. C. *Acta Crystallogr.* **1955**, *8*, 323.
(29) Rettenmeier, A.; Weidenhammer, K.; Ziegler, M. C. *Z. Anorg. Allg. Chem.* **1981**, *473*, 91.
(30) Atwood, J. L.; Bernal, I.; Calderazzo, F.; Canada, L. G.; Poli, R.; Rogers, R. D.; Veracini, C. A.; Vitali, D. *Inorg. Chem.* **1983**, *22*, 1797.

Contribution from the School of Chemistry and Biochemistry, Georgia Institute of Technology, Atlanta, Georgia 30332-0400

Reactivity of Pentacoordinate Ferrous Porphyrins with Exo-Bidentate Nitrogenous Bases. Mononuclear and Binuclear Complexes in Dynamic Equilibrium

Lawrence A. Bottomley* and Jean-Noel Gorce

The reaction of several exo-bidentate nitrogenous bases with thiocarbonyl(5,10,15,20-tetraphenylporphinato)iron(II) afforded six-coordinate mononuclear and binuclear porphyrin complexes in dynamic equilibrium. This reaction was carried out in halocarbon solvents and monitored both spectrally and electrochemically. Within the potential limits of the solvent/supporting electrolyte system, each complex underwent at least four separate electron-transfer reactions with retention of the thiocarbonyl ligand. An electron-transfer pathway is presented and supported by the combined results of infrared and electronic absorption spectra, variable-temperature proton NMR, variable-temperature electrochemical, and spectroelectrochemical experiments.

Introduction

The preparation and properties of binuclear metalloporphyrin complexes have been actively pursued since the structural characterization of hematin was reported.[1] Three general classes of

binuclear metalloporphyrins have been prepared: porphyrins linked at their periphery[2] by either covalent bonds[3,4] or ionic interactions,[5]

(1) Fleischer, E. B.; Srivastava, T. S. *J. Am. Chem. Soc.* **1969**, *91*, 2403.

porphyrins joined by multiple metal–metal bond,[6-9] and porphyrins linked by covalent bonds at the metal cores.[10] Binuclear iron porphyrins from the first and third classes are known. From the third group, single-atom-bridged iron porphyrin dimers have been prepared (with O, N, or C bridging moieties) and their physicochemical properties described.[11-13] Iron porphyrin dimers possessing multiatom bridges are not as well documented,[14] and their electrochemistry has not been reported.

(2) This class has recently been reviewed.[3] Notable examples of this class are the cofacial dimers of Collman and co-workers[4] (covalent attachment at the porphyrin periphery) and the crown ether derivatized complexes of Krishnan and co-workers[5] (ionic interactions at the periphery).

(3) Dolphin, D.; Hiom, J.; Paine, J. B. *Heterocycles* **1981**, *16*, 417.

(4) (a) Durand, R. R., Jr.; Bencosme, C. S.; Collman, J. P.; Anson, F. C. *J. Am. Chem. Soc.* **1983**, *105*, 2710. (b) Collman, J. P.; Bencosme, C. S.; Durand, R. R., Jr.; Kreh, R. P.; Anson, F. C. *J. Am. Chem. Soc.* **1983**, *105*, 2704. (c) Collman, J. P.; Bencosme, C. S.; Barnes, C. E.; Miller, B. D. *J. Am. Chem. Soc.* **1983**, *105*, 2699. (d) Collman, J. P.; Anson, F. C.; Barnes, C. E.; Bencosme, C. S.; Geiger, T.; Evitt, E. R.; Kreh, R. P.; Meier, K.; Pettman, R. B. *J. Am. Chem. Soc.* **1983**, *105*, 2694. (e) Collman, J. P.; Chong, A. O.; Jameson, G. B.; Oakley, R. T.; Rose, E.; Schmittou, E. R.; Ibers, J. A. *J. Am. Chem. Soc.* **1981**, *103*, 516. (f) Collman, J. P.; Marrocco, M.; Elliott, C. M.; L'Her, M. *J. Electroanal. Chem. Interfacial Electrochem.* **1981**, *124*, 113.

(5) (a) Thanabal, V.; Krishnan, V. *J. Am. Chem. Soc.* **1982**, *104*, 3643. (b) Thanabal, V.; Krishnan, V. *Inorg. Chem.* **1982**, *21*, 3606.

(6) The second class has been explored by the research teams of Collman,[7] Wayland,[8] and Ogoshi.[9]

(7) (a) Collman, J. P.; Barnes, C. E.; Collins, T. J.; Brothers, P. J. *J. Am. Chem. Soc.* **1981**, *103*, 7030. (b) Collman, J. P.; Barnes, C. E.; Woo, L. K. *Proc. Natl. Acad. Sci. U.S.A.* **1983**, *80*, 7684. (c) Collman, J. P.; Barnes, C. E.; Sweptson, P. N.; Ibers, J. A. *J. Am. Chem. Soc.* **1984**, *106*, 3500. (d) Collman, J. P.; Woo, L. K. *Proc. Natl. Acad. Sci. U.S.A.* **1984**, *81*, 2592. (e) Collman, J. P.; Prodolliet, J. W.; Leidner, C. R. *J. Am. Chem. Soc.* **1986**, *108*, 2916.

(8) Wayland, B. B.; Newman, A. R. *Inorg. Chem.* **1981**, *20*, 3093.

(9) Ogoshi, H.; Setsune, J.; Yoshida, Z. *J. Am. Chem. Soc.* **1977**, *99*, 3869.

(10) The last class of complexes is best illustrated by the oxo-bridged dimers prepared by West and co-workers: (a) Liston, D. J.; Murray, K. S.; West, B. O. *J. Chem. Soc., Chem. Commun.* **1982**, 1109. (b) Liston, D. J.; Kennedy, B. J.; Murray, K. S.; West, B. O. *Inorg. Chem.* **1985**, *24*, 1561.

(11) (a) Felton, R. H.; Owens, G. S.; Dolphin, D.; Fajer, J. *J. Am. Chem. Soc.* **1971**, *93*, 6332. (b) Felton, R. H.; Owens, G. S.; Dolphin, D.; Forman, A.; Barry, D. C.; Fajer, J. *Ann. N.Y. Acad. Sci.* **1973**, *206*, 504. (c) Phillippi, M. A.; Goff, H. M. *J. Am. Chem. Soc.* **1979**, *101*, 7641. (d) Kadish, K. M.; Larson, G.; Lexa, D.; Momenteau, M. *J. Am. Chem. Soc.* **1975**, *97*, 282. (e) Phillippi, M. A.; Shimomura, E. T.; Goff, H. M. *Inorg. Chem.* **1981**, *20*, 1322. (f) Phillippi, M. A.; Goff, H. M. *J. Am. Chem. Soc.* **1982**, *104*, 6062. (g) Chang, D.; Cocolios, P.; Wu, Y. T.; Kadish, K. M. *Inorg. Chem.* **1984**, *23*, 1629. (h) Bottomley, L. A.; Ercolani, C.; Gorce, J.-N.; Pennesi, G.; Rossi, G. *Inorg. Chem.* **1986**, *25*, 2338–2342.

(12) (a) Kadish, K. M.; Chang, J. S.; Cohen, I. A.; Summerville, D. *ACS Symp. Ser.* **1977**, *No. 38*, 65. (b) Kadish, K. M.; Rhodes, R. K.; Bottomley, L. A.; Goff, H. M. *Inorg. Chem.* **1981**, *20*, 3195. (c) Kadish, K. M.; Bottomley, L. A.; Brace, J. G.; Winograd, W. J. *J. Am. Chem. Soc.* **1980**, *102*, 4341. (d) Scheidt, W. R.; Summerville, D.; Cohen, I. A. *J. Am. Chem. Soc.* **1976**, *98*, 6623. (e) Summerville, D.; Cohen, I. A. *J. Am. Chem. Soc.* **1976**, *98*, 1747. (f) Schick, G. A.; Bocian, D. F. *J. Am. Chem. Soc.* **1980**, *102*, 7982. (g) Schick, G. A.; Bocian, D. F. *J. Am. Chem. Soc.* **1983**, *105*, 1830. (h) Schick, G. A.; Findsen, E. W.; Bocian, D. F. *Inorg. Chem.* **1982**, *21*, 2885. (i) Bottomley, L. A.; Garrett, B. B. *Inorg. Chem.* **1982**, *21*, 1260. (j) Bottomley, L. A.; Gorce, J.-N.; Goedken, V. L.; Ercolani, C. *Inorg. Chem.* **1985**, *24*, 3733–3737.

(13) (a) Battioni, J. P.; Lexa, D.; Mansuy, D.; Saveant, J. M. *J. Am. Chem. Soc.* **1983**, *105*, 207. (b) Lancon, D.; Kadish, K. M. *Inorg. Chem.* **1984**, *23*, 3942. (c) Goedken, V. L.; Deakin, M. R.; Bottomley, L. A. *J. Chem. Soc., Chem. Commun.* **1982**, 607.

(14) Caughey and co-workers[15] prepared a μ-hydrazido iron porphyrin dimer upon the reaction of the μ-oxo dimer with hydrazine hydrate under a CO atmosphere. Kessel and Hendrickson[16] reported the dimerization of iron porphyrins using a series of hydroquinone dianions as bridging ligands. Elliott and co-workers[17] have recently isolated an iron(III) porphyrin dimer with *trans*-dicyanoethylenedithiolate as the bridging moiety.

(15) Caughey, W. S.; Barlow, C. H.; O'Keeffe, D. H.; O'Toole, M. C. *Ann. N.Y. Acad. Sci.* **1973**, *206*, 296.

(16) Kessel, J. L.; Hendrickson, D. N. *Inorg. Chem.* **1980**, *19*, 1983.

(17) Elliott, C. M.; Akabori, K.; Anderson, O. P.; Schauer, C. K.; Hatfield, W. E.; Sczaniecki, P. B.; Mitra, S.; Spartalian, K. *Inorg. Chem.* **1986**, *25*, 1891.
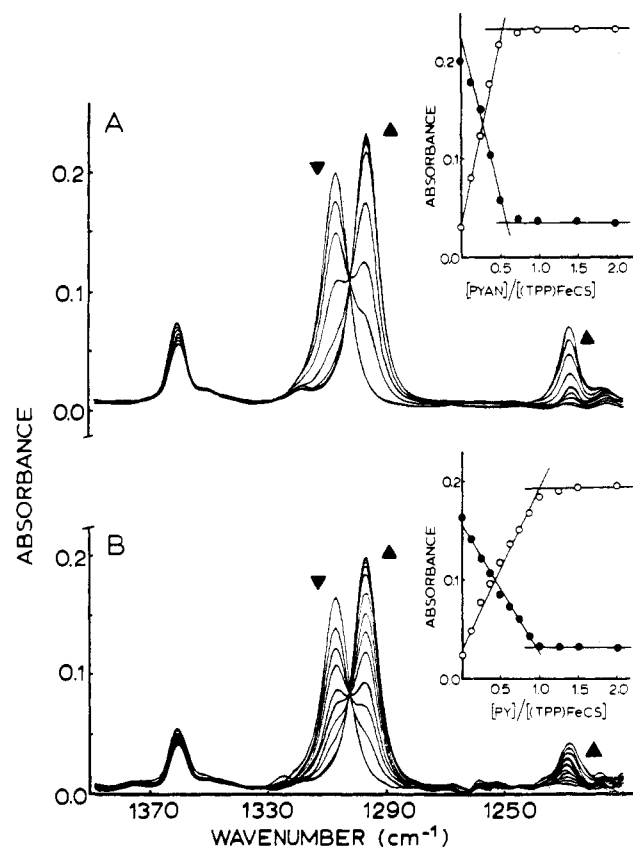
Figure 1. Infrared data acquired during the titration of (TPP)FeCS in benzene with (A) PYAN and (B) py. The inset plots depict the changes in absorbance versus the molar ratio of (A) PYAN/(TPP)FeCS and (B) py/(TPP)FeCS at 1307 cm^{-1} (closed circles) and at 1294 cm^{-1} (open circles).

The paucity of available binuclear multiatom-bridged iron porphyrin complexes is due to the facility with which both ferric and ferrous porphyrins undergo diadduct formation. Consequently, polymerization occurs when most mononuclear iron porphyrins are treated with exo-bidentate Lewis bases.[18-22] This reactivity has recently been exploited by Collman and co-workers[22] in their preparation of novel metalloporphyrin-based conducting polymers. These materials were of special interest because the conductive pathway did not involve the porphyrin ring π electrons.

Two approaches for inhibiting polymerization can be envisioned. One is to sterically prevent the formation of a six-coordinate iron center. A variety of porphyrins have been invented that possess a high degree of steric hindrance on one side of the porphyrin plane. Some of these (e.g. the "pocket"[23] and "capped" porphy-

(18) Wang and Brinigan[19] have shown that iron(II) protoporphyrin forms an insoluble polymer with 4,4'-bipyridyl in aqueous solution. Attempts by Cohen and Ostfeld[20a] to dimerize iron(III) tetraphenylporphyrin using imidazolate as a bridging ligand also led to the polymeric product. Scheidt and Reed[20b-d] have characterized the μ-imidazolato polymeric products for several different metalloporphyrins. Montalvo and Davis[21] observed a precipitate forming upon the reaction of 4,4'-bipyridyl and either iron(II) hematoporphyrin or iron(II) protoporphyrin IX in aqueous solution.

(19) Wang, J. H.; Brinigan, W. S. *Proc. Natl. Acad. Sci. U.S.A.* **1960**, *46*, 958.

(20) (a) Cohen, I. A.; Ostfeld, D. *ACS Symp. Ser.* **1974**, *No. 5*, 221. (b) Landrum, J. T.; Reed, C. A.; Hatano, K.; Scheidt, W. R. *J. Am. Chem. Soc.* **1978**, *100*, 3232. (c) Landrum, J. T.; Hatano, K.; Scheidt, W. R.; Reed, C. *J. Am. Chem. Soc.* **1980**, *102*, 6729. (d) Landrum, J. T.; Grimmett, D.; Haller, K. J.; Scheidt, W. R.; Reed, C. A. *J. Am. Chem. Soc.* **1981**, *103*, 2640.

(21) Montalvo, J. G.; Davis, D. G. *Anal. Lett.* **1969**, *2*, 341.

(22) (a) Collman, J. P.; McDevitt, J. T.; Yee, G. T.; Leidner, C. R.; McCullough, L. G.; Little, W. A.; Torrance, J. B. *Proc. Natl. Acad. Sci. U.S.A.* **1986**, *83*, 4581. (b) Collman, J. P.; McDevitt, J. T.; Yee, G. T.; Zisk, M. B.; Torrance, J. B.; Little, W. A. *Synth. Met.* **1986**, *15*, 129. (c) Collman, J. P.; McDevitt, J. T.; Leidner, C. R.; Yee, G. T.; Torrance, J. B.; Little, W. A. *J. Am. Chem. Soc.* **1987**, *109*, 4606.

rins[24]) have proven effective in preventing the formation of six-coordinate iron centers in the presence of excess monodentate nitrogenous bases and presumably could be used to prepare binuclear iron porphyrins with multiatom bridges.[25] A second approach for preventing polymerization (and the one investigated herein) is via a blocking group. Treatment of pentacoordinate iron porphyrins that possess a nonlabile axial ligand with a stoichiometric amount of the exo-bidentate ligand may yield a binuclear multiatom-bridged complex.

Our recent studies of chalcocarbonyl iron porphyrins[27,28] have shown that the diatomic ligand is indeed nonlabile when these porphyrins are exposed to secondary amines, regardless of the valence of the iron core or the charge on the porphyrin ring. Thus, the chalcocarbonyl iron porphyrins appeared to be ideal candidates for the formation of binuclear multiatom-bridged complexes. In this paper, we present evidence for the dimerization of (TPP)-FeCS[31] in the presence of a variety of exo-bidentate nitrogenous bases.

Experimental Section

Materials. Thiocarbonyl(5,10,15,20-tetraphenylporphyrinato)iron(II), (TPP)FeCS, was synthesized by the method of Buchler[29] and Mansuy[30] with the modifications previously detailed.[27] All nitrogenous bases were purchased and used as received from Aldrich Chemical Co. Tetra-*n*-butylammonium perchlorate (Eastman Chemical Co.) was recrystallized three times from absolute ethanol and vacuum-dried for 24 h prior to use. 1,2-Dichloroethane and dichloromethane were each extracted from concentrated sulfuric acid and distilled water. The extracts were fractionally distilled over phosphorus pentoxide under a nitrogen atmosphere.

Instrumentation. Spectroelectrochemical data were obtained with a Tracor Northern 6050 spectrometer coupled to a Tracor Northern 1710 multichannel analyzer with a Data Systems Design dual-floppy-disk storage device. Electron-transfer reactions were initiated and controlled by an IBM Instruments Model EC225A polarographic system. Infrared spectra were obtained with a Nicolet 5DXB FT-IR spectrometer. Hard copies of all spectra were obtained with a Hewlett-Packard 7470A digital plotter. Voltammetric experiments were carried out as previously reported.[27,28] Variable-temperature ^{1}H NMR spectra were obtained on a Bruker WM-300 spectrometer.

Results and Discussion

Spectral Characterization of Mononuclear and Binuclear Complexes. Addition of L-L[31] to solutions of (TPP)FeCS produced substantial red shifts in the electronic spectrum; the Soret band at 407 nm shifted to 422 nm, the α band at 522 nm shifted to 542 nm, and the β band shifted from 548 to 580 nm. The spectrum of the complex is that characteristic of six-coordinate chalcocarbonyl iron porphyrins.[27-30] Analysis of the spectral changes as a function of [L-L] indicated that the complexation reaction involved two molecules of (TPP)FeCS per molecule of L-L.
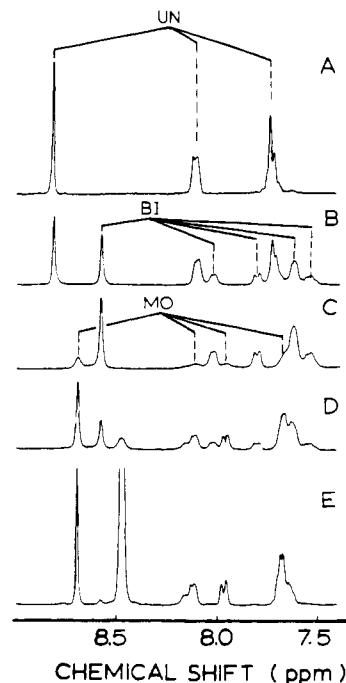
Figure 2. ^{1}H NMR spectra acquired during the titration of 2.11 mM (TPP)FeCS in CDCl$_3$ under isothermal conditions (−55 °C) at the following molar ratios of PYAN to (TPP)FeCS: (A) 0.00; (B) 0.23; (C) 0.55; (D) 1.25; (E) 7.37. Resonances designated with UN, BI, and MO refer to the porphyrin proton resonances of the uncomplexed (TPP)FeCS, the binuclear complex [(TPP)FeCS]$_2$(L-L), and the mononuclear complex (TPP)FeCS(L-L), respectively.

Verification that the reaction with L-L did not displace the thiocarbonyl group was given by the infrared spectrum of the complex. Addition of L-L to a benzene solution of (TPP)FeCS shifted the C≡S stretch from 1307 to 1294 cm^{-1} (or 1300 cm^{-1} when L-L was PYZ or DABCO). Analysis of the absorbance changes at both 1307 and 1294 cm^{-1} as a function of [L-L] indicated that the complexation reaction involved two molecules of (TPP)FeCS per molecule of L-L. A typical data set is displayed in Figure 1 for L-L = PYAN. For ready comparison, a data set for L = pyridine is included in this figure. When they were taken collectively, the results of both spectral titration studies suggested that (1) the Fe−CS bond remains intact even in the presence of a large excess of L-L, (2) the reaction of (TPP)FeCS with L-L produced six-coordinate complexes rather than polymeric material with [−Fe−L−L−Fe−L−L−]$_n$ or [−S−C−Fe−L−L−Fe−]$_n$ repeating units, and (3) only half the [L-L] is required to convert five-coordinate (TPP)FeCS to a six-coordinate complex as compared to [L].

In general, the ^{1}H NMR spectrum of ferrous porphyrins is complicated by rapid exchange when axial ligands are present.[30,32-34] Mansuy and co-workers[30] have shown that a single exchange process existed for (TPP)FeCS(L) complexes for a limited number of nitrogenous bases, i.e.

$$S{=}C{-}\overset{|}{\underset{|}{Fe}} + L \;\rightleftarrows\; S{=}C{-}\overset{|}{\underset{|}{Fe}}{-}L \qquad (1)$$
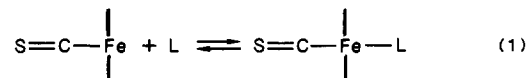
Note that the vertical bonds denote the porphyrin ring. We have

(23) (a) Collman, J. P.; Brauman, J. I.; Collins, T. J.; Iverson, B.; Sessler, J. L. *J. Am. Chem. Soc.* **1981**, *103*, 2450. (b) Collman, J. P.; Basolo, F.; Bunnenbury, E.; Collins, T. J.; Dawson, J. H.; Ellis, P. E.; Marroco, M. L.; Moscowitz, A.; Sessler, J. L.; Szymanski, T. *J. Am. Chem. Soc.* **1981**, *103*, 5636.

(24) (a) Baldwin, J. E.; Almog, J.; Dyer, R. L.; Peters, M. *J. Am. Chem. Soc.* **1975**, *97*, 226. (b) Almog, J.; Baldwin, J. E.; Huff, J. *J. Am. Chem. Soc.* **1975**, *97*, 227. (c) Ellis, P. E.; Linard, J. E.; Szymanski, T.; Budge, R. D.; Basolo, F. *J. Am. Chem. Soc.* **1980**, *102*, 1889.

(25) This reaction pathway has been demonstrated by Uemori and co-workers[26] in their preparation of binuclear cobalt porphyrins.

(26) Uemori, Y.; Nakatsubo, A.; Imai, H.; Nakagamo, s.; Kyuno, E. *Inorg. Chim. Acta* **1985**, *108*, 217.

(27) Bottomley, L. A.; Deakin, M. R.; Gorce, J.-N. *Inorg. Chem.* **1984**, *23*, 3563.

(28) (a) Gorce, J.-N.; Bottomley, L. A. *Inorg. Chem.* **1985**, *24*, 1431. (b) Gorce, J.-N. *J. Electrochem. Soc.* **1984**, *131*, 35C.

(29) Buchler, J. W.; Kobisch, W.; Smith, P. D.; Tonn, B. *Z. Naturforsch., B: Anorg. Chem., Org. Chem.* **1978**, *33B*, 1371.

(30) (a) Mansuy, D.; Battioni, J.-P.; Chottard, J.-C. *J. Am. Chem. Soc.* **1978**, *100*, 4311. (b) Battioni, J.-P.; Chottard, J. C.; Mansuy, D. *Inorg. Chem.* **1982**, *21*, 2056.

(31) Abbreviations used: L = monodentate nitrogenous base; L-L = exo-bidentate nitrogenous base; TPP = 5,10,15,20-tetraphenylporphinato dianion; EtCl$_2$ = 1,2-dichloroethane; PYZ = pyrazine; PYAN = 1,2-bis(4-pyridyl)ethane; PYEN = 1,2-bis(4-pyridyl)ethylene; BIPY = 4,4′-bipyridyl dihydrate; DABCO = 1,4-diazabicyclo[2.2.2]octane; py = pyridine; 4-pic = 4-picoline.

(32) (a) La Mar, G. N.; Walker, F. A. In *The Porphyrins*; Dolphin, D., Ed.; Academic: New York, 1979; Vol. IV, pp 61-157. (b) La Mar, G. N. In *Biological Applications of Magnetic Resonance*; Shulman, R. G., Ed.; Academic: New York, 1979; pp 305-349 and references therein.

(33) Goff, H. M. In *Iron Porphyrins*; Lever, A. B. P., Gray, H. B., Eds.; Addison-Wesley: Reading, MA, 1983; Part 1, Chapter 4, and references therein.

(34) (a) Janson, T. R.; Katz, J. J. In *The Porphyrins*; Dolphin, D., Ed.; Academic: New York, 1979; Vol. IV, pp 1-59. (b) Morishima, I.; Ogawa, S.; Inubushi, T.; Iizuka, T. *Adv. Biophys.* **1978**, *11*, 217. (c) Morrow, J. S.; Gurd, F. R. N. *CRC Crit. Rev. Biochem.* **1975**, *3*, 221 and references therein.

Table I. Proton NMR Chemical Shifts[a] for Monomeric and Dimeric Thiocarbonyl Iron Porphyrin Complexes

| complex	porphyrin			ligand[b]		
	pyrrole	ortho	meta, para	α	β	γ
(TPP)FeCS	8.83 (s)	8.13	7.72			
(TPP)FeCS(py)	8.70 (s)	8.12	7.65	1.65 (s)	5.23 (s)	6.14 (s)
		7.97				
(TPP)FeCS(4-pic)	8.68 (s)	8.12	7.66	1.50 (s)	5.00 (s)	1.23 (s)
		7.97				
(TPP)FeCS(PYAN)	8.70 (s)	8.12	7.67	1.55 (s)	5.01 (s)	1.79 (s)
		7.97		8.17 (s)	6.44 (s)	1.95 (s)
(TPP)FeCS(PYEN)	8.70 (s)	8.12	7.69	1.67 (s)	5.27 (s)	6.12 (s)
		7.97		8.34 (s)	6.89 (s)	6.21 (s)
(TPP)FeCS(BIPY)	8.72 (s)	8.12	7.70	1.78 (s)	5.51 (s)	
		7.98		8.54 (s)	6.53 (s)	
(TPP)FeCS(DABCO)	8.74 (s)	8.10 (s)	7.71	−3.40 (s)		
				0.78		
(TPP)FeCS(PYZ)	8.72 (s)	8.08	7.67	0.82		
		8.0		6.42		
py				8.61	7.28	7.58
4-pic				8.44	7.12	2.34 (s)
PYAN				8.44	7.07	2.91 (s)
PYEN				8.64	7.37	7.21 (s)
BIPY				8.76	7.54	
DABCO				2.81 (s)		
PYZ				8.64 (s)		
[(TPP)FeCS]₂(PYAN)	8.58 (s)	8.02 (s)	7.63 (s)	1.32 (d)	4.62 (d)	0.78 (s)
		7.81 (d)	7.54 (s)			
[(TPP)FeCS]₂(PYEN)	8.58 (s)	8.01 (s)	7.63 (s)	1.39 (d)	4.82 (d)	5.10 (s)
		7.82 (d)	7.54 (s)			
[(TPP)FeCS]₂(BIPY)	8.54 (s)	8.02 (s)	7.62 (s)	1.30 (d)	4.42 (d)	
		7.82 (d)	7.52 (s)			
[(TPP)FeCS]₂(DABCO)	8.41 (s)	7.84 (d)	7.60	−5.28 (s)		
		7.60	7.51			
[(TPP)FeCS]₂(PYZ)	8.41 (s)	7.83 (s)	7.60	−0.17 (s)		
		7.60	7.52			

[a] Chemical shifts referenced against $CHCl_3$ proton and determined at −55 °C. Except where noted within parentheses, the chemical shifts listed were measured at the midpoint of complex multiplets. [b] Denotes carbon position relative to the nitrogen donor atom.

confirmed this observation utilizing several substituted pyridines and quinuclidine.

In the presence of exo-bidentate ligands, additional exchange processes were observed. The chemical shifts of the porphyrin proton resonances at various temperatures and ligand to porphyrin molar ratios reflected three species in equilibrium: uncomplexed, mononuclear, and binuclear porphyrins. Resonances of ligand protons were observed for free L-L and L-L in the binuclear complex, and two different resonances were observed for L-L in the mononuclear complex: one set for the bound site and another for the unbound end of the ligand.

Our method for assigning the resonance to a specific proton on the porphyrin is illustrated in Figures 2 and 3 for spectra acquired at varying molar ratios of PYAN:(TPP)FeCS at −55 °C. In the absence of L-L, the resonance of the pyrrole protons was observed at 8.83 ppm (see Figure 2A) in agreement with the results of Mansuy and co-workers.[30] As the molar ratio of PYAN:(TPP)FeCS was increased to 0.5, a resonance at 8.58 ppm increased in intensity in proportion to the decrease in intensity of the resonance at 8.83 ppm (see Figure 2B). At molar ratios greater than 0.50, the resonance of the uncomplexed porphyrin disappeared and a resonance due to the mononuclear complex grew at 8.70 ppm. The intensity at 8.70 ppm increased with a proportionate decrease in the intensity of the resonance at 8.58 ppm (see Figure 2C−E). The latter resonance (due to the binuclear complex) persisted until the molar ratio of PYAN:(TPP)FeCS exceeded 7.5. The intensities of the resonances of the ortho, meta, and para protons were also dependent upon [PYAN] (see Figure 2).

Similar trends were observed for ligand resonances as illustrated in Figure 3. For example, the resonance for the proton on the β-carbon (relative to the N-donor atom) of free PYAN was 7.07 ppm. No detectable amount of free PYAN was observed until the PYAN:(TPP)FeCS molar ratio exceeded 1. At a molar ratio of 0.23 (Figure 3B) the resonance of the β-proton in the binuclear complex was observed at 4.62 ppm. Its intensity was inversely
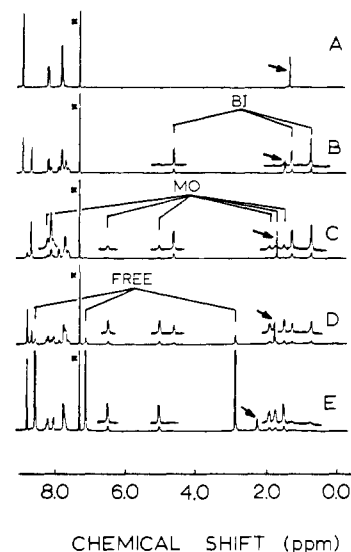
Figure 3. ¹H NMR spectra acquired under the conditions given in the caption for Figure 2. Resonances marked with an arrow are due to H_2O, and those marked with X are due to $CHCl_3$. Resonances designated with BI, MO, and FREE refer to the ligand resonances of the binuclear complex [(TPP)FeCS]₂(L-L), the mononuclear complex (TPP)FeCS-(L-L), and the free ligand, respectively.

proportional to the intensity of the β-protons in the mononuclear complex (see Figure 3B−E) at 5.01 (on the end bound to the iron) and 6.44 ppm (on the unbound end). The relative intensities of the α- and γ-protons were also dependent on [PYAN]. Similar studies were carried out with other exo-bidentate ligands with comparable results as summarized in Table I. Note that the term γ refers either to the protons on the alkyl linking group of PYAN and PYEN or to the protons at the 4-position of the monodentate ligands py or 4-pic.
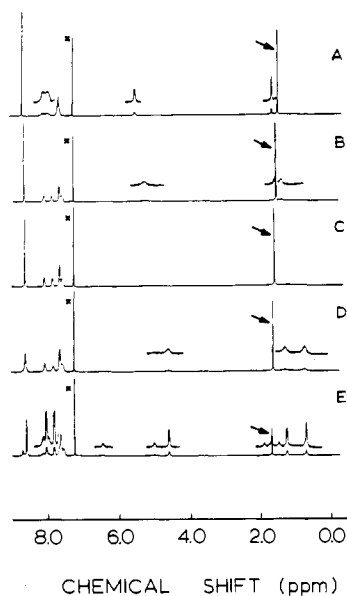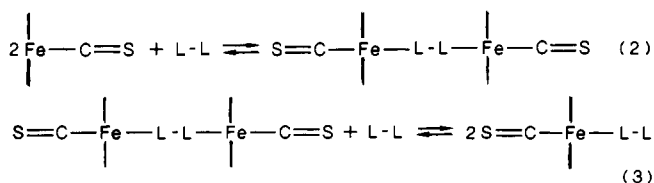
Figure 4. ^{1}H NMR spectra of 2.11 mM (TPP)FeCS in CDCl$_3$ containing a molar ratio of PYAN/(TPP)FeCS = 0.55. Spectra were taken at the following temperatures: (A) 25 °C; (B) 0 °C; (C) –20 °C; (D) –40 °C; (E) –55 °C. Resonances marked with an arrow are due to H$_2$O, and those marked with X are due to CHCl$_3$.

From the observations acquired at –55 °C, we concluded (1) no uncomplexed porphyrin was observed at greater than stoichiometric levels of ligand, illustrating the high affinity of the porphyrin for coordination by nitrogenous bases, (2) unique resonances were observed for the uncomplexed, mononuclear, and binuclear porphyrins as well as for the free ligand, and (3) at this temperature, the rates of exchange were slower than the time scale of the experiment.

The last conclusion was verified by a variable-temperature study. Figure 4 depicts ^{1}H NMR spectra acquired at temperatures ranging from +25 to –55 °C on a solution containing a molar ratio PYAN:(TPP)FeCS of 0.55. At –55 °C (Figure 4E) the spectrum contained resonances of only the binuclear and mononuclear complexes in 10:1 relative abundance. As the temperature was increased, the porphyrin resonances broadened and shifted downfield. At 25 °C, the pyrrole proton resonance was observed as a singlet at 8.66 ppm, the ortho protons were an unresolved doublet with maxima at 8.06 and 7.92 ppm, and the meta and para protons were unresolved at 7.65 ppm.

A temperature dependence was also observed for the ligand protons. The sharp, well-resolved resonances for the ligand protons observed at –55 °C coalesced near –40 °C to three resonances of equal integration at 0.81, 1.37, and 4.62 ppm. As the temperature was elevated to 25 °C, the resonance of the ligand protons collapsed (see Figure 4C) and then reappeared (see Figure 4A,B), shifting downfield with increasing temperature (except that of the α-protons, which remained collapsed over the range –20 to +25 °C). Comparable results were obtained for each L-L investigated. The observed chemical shifts as a function of temperature suggested the following equilibria operative for exobidentate nitrogenous bases:

$$2\,\overset{|}{\underset{|}{Fe}}{-}C{=}S + L\text{-}L \rightleftharpoons S{=}C{-}\overset{|}{\underset{|}{Fe}}{-}L\text{-}L{-}\overset{|}{\underset{|}{Fe}}{-}C{=}S \quad (2)$$

$$S{=}C{-}\overset{|}{\underset{|}{Fe}}{-}L\text{-}L{-}\overset{|}{\underset{|}{Fe}}{-}C{=}S + L\text{-}L \rightleftharpoons 2\,S{=}C{-}\overset{|}{\underset{|}{Fe}}{-}L\text{-}L \quad (3)$$

Thus, the binuclear complex was present in solution only at temperatures less than –40 °C. This is not in conflict with the results of the electronic absorption and infrared spectral results presented above. The results obtained by these two techniques accurately recorded changes in the coordination state of the iron
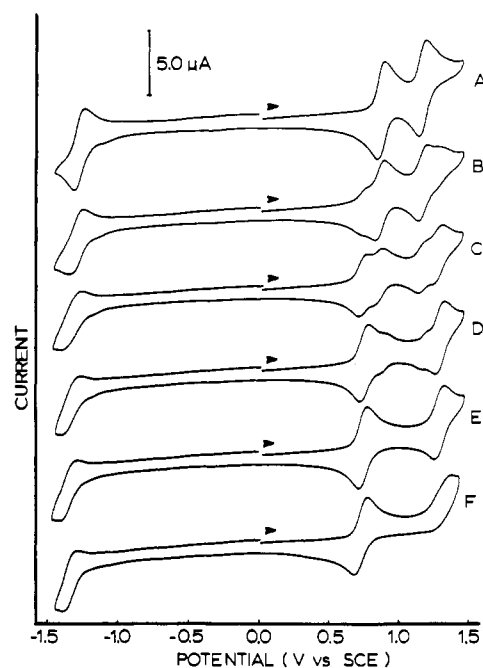
Figure 5. Cyclic voltammetric data obtained during the titration of (TPP)FeCS with PYAN at a potential sweep rate of 200 mV s^{-1}. Voltammograms were recorded at the following molar ratios of PYAN/(TPP)FeCS: (A) 0.000; (B) 0.125; (C) 0.250; (D) 0.375; (E) 0.500; (F) 0.750.

but were insensitive to the dynamics of the mononuclear/binuclear equilibrium. The electronic absorption experiments recorded the conversion of the five-coordinate (TPP)FeCS to the six-coordinate species (TPP)FeCS(L-L) or [(TPP)FeCS]$_2$(L-L) because the electronic absorption spectra of the two six-coordinate complexes are identical. Similarly, the infrared absorption experiments documented the conversion of (TPP)FeCS to either (TPP)FeCS(L-L) or [(TPP)FeCS]$_2$(L-L) because, in these experiments, the intensity and position of the $\nu_{C=S}$ vibration is sensitive only to the presence of a nitrogenous base in the axial position trans to the CS moiety. Thus, in both sets of experiments, absorbance changes terminated after the L-L:(TPP)FeCS ratios exceeded 0.5 without documenting the binuclear to mononuclear interconversion readily detectable by variable-temperature NMR.

Electrochemical Studies. Trace A of Figure 5 depicts a typical cyclic voltammogram of (TPP)FeCS in the absence of either L or L-L recorded at ambient temperature. Three of the four redox couples accessible within the potential range of EtCl$_2$/0.1 M TBAP are shown.[35] Traces B–E illustrate the CV's obtained after the sequential addition of L-L (in this case L-L = PYAN) to the solution. In this sequence, the two electrooxidation processes and one electroreduction process were replaced by three new processes, which corresponded to the electrolysis of the six-coordinate porphyrin complex. Trace E was taken when [L-L] = 2-[(TPP)FeCS] and showed that no pentacoordinate iron porphyrin species was present in solution. Analysis of the current–voltage curves obtained for each process taken over the potential sweep rate range of 20 mV s^{-1} to 10 V s^{-1} yielded current–voltage–sweep-rate trends consistent with theory for quasi-reversible electron transfers. Coulometric experiments confirmed the transfer of one electron per Fe porphyrin molecule. At excess [L-L], the second oxidation process is complicated by the catalytic oxidation of L-L by the porphyrin dication. Titrations monitored by dif-

(35) The electroreductive behavior of (TPP)FeCS and (TPP)FeCS(L) in EtCl$_2$ was similar to that observed in dimethylformamide by Battioni and co-workers.[13a] For (TPP)FeCS, the first reduction process occurred at an $E_{1/2}$ value of –1.29 V and is reversible on the cyclic voltammetric time scale. The second process, chemically coupled to the first, occurred at an E_p value of –1.62 V (measured at a sweep rate of 200 mV s^{-1}). Protonation of the thiocarbonyl group occurred very rapidly after the electron transfer.

Table II. Half-Wave Potentials[a] for Electrode Reactions of [(TPP)FeCS]₂(L-L) and (TPP)FeCS(L-L) Complexes

| | redox reacn | | |
ligand identity	eq 6, 10	eq 5, 9	eq 4, 8
none	−1.29	0.85	1.16
PYZ	−1.35	0.76	1.31
BIPY	−1.37	0.73	1.28
PYAN	−1.35	0.72	1.27
PYEN	−1.37	0.72	1.27
DABCO	−1.36	b	b

[a] Potentials are in volts versus the SCE. [b] Ligand oxidation occurred prior to the oxidation of the complex.

ferential pulse voltammetry (in the manner previously described[27,28]) indicated that (1) at a molar ratio of 2:1 (TPP)Fe-CS:L-L all of the electrode reactant is complexed and (2) all electrogenerated products of (TPP)FeCS were coordinated by an identical number of molecules of L-L.

Identical experiments with all of the other exo-bidentate ligands used gave comparable results. Spectroelectrochemical experiments confirmed the chemical reversibility of both oxidation processes as well as the number of electrons transferred.[36] Half-wave potentials for all three electron-transfer reactions are listed in Table II as a function of the identity of L-L.

In light of the NMR results, the electrochemistry of (TPP)FeCS was also investigated as a function of temperature. Due to the limited temperature range of $EtCl_2$, CH_2Cl_2 was used as the solvent for this study. Over the range from +25 to −77 °C, two oxidation processes were observed (at $E_{1/2} = 0.84$ and 1.16 V) with current–potential dependences on scan rate that were comparable to those observed in $EtCl_2$. For example, at −77 °C, the peak potential separations (at a potential sweep rate of 20 mV s⁻¹) were 41 and 43 mV for the first and second oxidation processes, respectively. The theoretical value[37] for a reversible electron-transfer process at this temperature is 37.5 mV. The potential differences (at a potential sweep rate of 20 mV s⁻¹) between the peak potentials and the potentials at half peak current, $E_p - E_{p/2}$, were 42 and 45 mV, respectively. Theory[37] predicts a value of 37.2 mV at this temperature. Peak potential separations and $E_p - E_{p/2}$ values recorded at −77 °C increased slightly with increasing scan rate. These small deviations from theory are probably due to uncompensated solution resistance, since at all potential sweep rates, $E_{1/2}$ values remained constant, anodic peak currents were proportional to the square root of the potential sweep rate, and the peak current ratios ($i_{p,c}/i_{p,a}$) were equal to unity.

When cyclic and differential pulse voltammograms were acquired in the presence of L-L, only two electrooxidation processes were observed, even under conditions where the binuclear complex was the predominant species in solution. For example, voltammograms recorded on a 1.0 mM solution of (TPP)FeCS that was 0.50 mM in PYZ at −77 °C contained two processes with half-wave potentials of 0.76 and 1.31 V, respectively. The peak potential separations (at 20 mV s⁻¹) were 39 and 41 mV for the first and second oxidation processes, respectively. The potential differences $E_p - E_{p/2}$ were 42 and 45 mV, respectively (at 20 mV s⁻¹). Peak potential separations and $E_p - E_{p/2}$ values recorded at −77 °C increased slightly with increasing scan rate. The values observed for both of these peak-shape parameters compared favorably with the values obtained in the absence of L-L. Also, $E_{1/2}$ values remained constant and the peak current ratios were equal to unity over all potential sweep rates investigated. The anodic peak currents were both proportional to the square root of the potential sweep rate and were equal in magnitude to those obtained in the absence of L-L. Differential pulse voltammograms acquired at −77 °C in the presence of L-L were comparable in peak amplitude and width to those obtained in the absence of L-L.

Scheme I
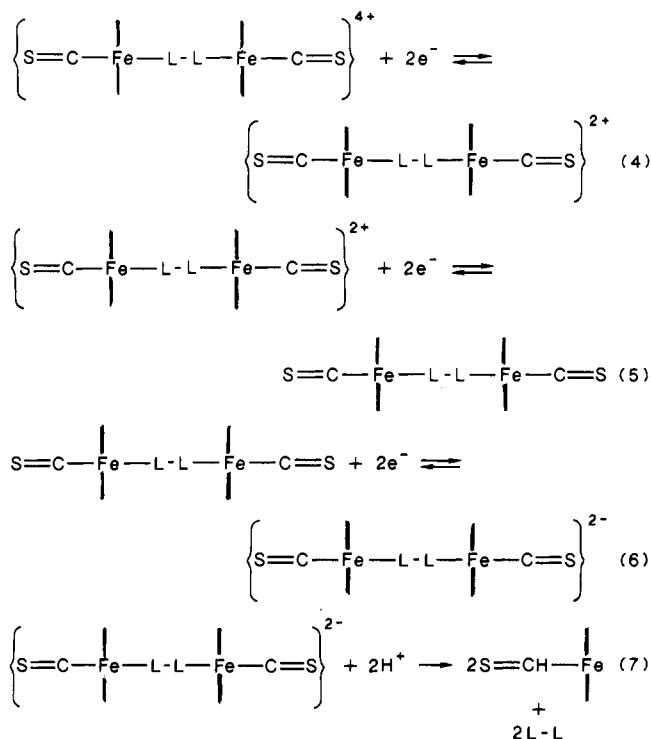
Scheme II
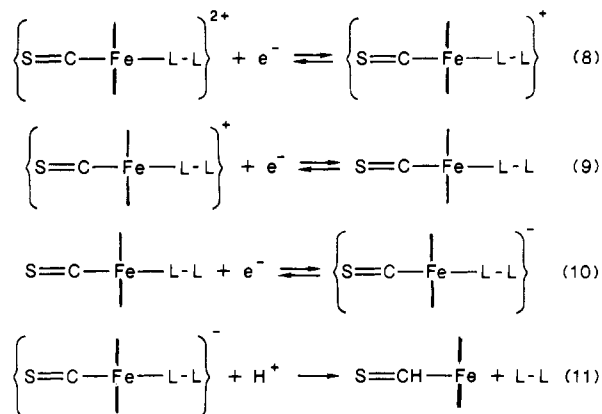
Several workers have investigated electron transfer to and from molecules with both interacting[37–42] and noninteracting[42,43] multiple redox centers. When a molecule contains two or more strongly interacting redox centers, multiple electron-transfer processes result. As this interaction decreases, the potential separation between these processes decreases. Richardson and Taube[42] have shown that the peak shape and peak magnitude are reliable indicators of the extent of redox center interaction. Flanagan and co-workers[43] have shown that when molecules contain two or more noninteracting redox centers, the current–potential curve will possess the same shape as that of a molecule with only a single redox center. Careful analysis of the cyclic voltammetric and differential pulse data sets indicated that the redox reactivity of the binuclear complexes investigated herein involve the simulta-

(36) The spectra of the iron(III) cationic species and iron(III) radical dicationic species have previously been published.[14,27]

(37) Nicholson, R.; Shain, I. *Anal. Chem.* **1964**, *36*, 706.

(38) Ammar, F.; Saveant, J. M. *J. Electroanal. Chem. Interfacial Electrochem.* **1973**, *47*, 115–125, 215–221.

(39) Polcyn, D. S.; Shain, I. *Anal. Chem.* **1966**, *38*, 370.

(40) Myers, R. L.; Shain, I. *Anal. Chem.* **1969**, *41*, 980.

(41) Yap, W. T.; Durst, R. A. *J. Electroanal. Chem. Interfacial Electrochem.* **1981**, *130*, 3.

(42) Richardson, D. E.; Taube, H. *Inorg. Chem.* **1981**, *20*, 1278.

(43) Flanagan, J. B.; Margel, S.; Bard, A. J.; Anson, F. C. *J. Am. Chem. Soc.* **1978**, *100*, 4248.

neous transfer of two electrons per complex, one from each noninteracting center in the molecule.

Electron-Transfer Pathway. On the basis of the combined results from the various spectral and electrochemical experiments presented above, two electron-transfer pathways are proposed. Under conditions where the binuclear complex is the predominant species in solution (stoichiometric levels of L-L and low temperatures), electron-transfer reactivity follows the sequence given in Scheme I. In this scheme, each redox site in the binuclear complex does not interact with the other. The sites of oxidation and reduction are identical with those proposed for the mononuclear complex, as given below. This scheme tacitly assumes that the rates of exchange among the free, mononuclear, and binuclear complexes (see eq 2 and 3) are not enhanced by the application of a potential field. Scheme II depicts the electron-transfer pathway proposed for the mononuclear complexes (TP-P)FeCS(L-L) and is identical with that previously proposed for (TPP)FeCS(L)[27] and (TPP)FeCSe(L).[28] This pathway is operative in the presence of excess L-L over all temperatures.

For both binuclear and mononuclear complexes, the first oxidation processes (eq 5 and 9) are metal-centered, formally producing six-coordinate thiocarbonyl ferric porphyrin complexes. The second oxidation processes (eq 4 and 8) are ring-centered, generating six-coordinate ferric porphyrin cation radicals. The first reduction processes (eq 6 and 10) are ring-centered, initially generating six-coordinate ferrous porphyrin anion radical complexes. The thiocarbonyl group in these species is rapidly attacked by protons to form either a five- or six-coordinated thioformyl ferrous porphyrin complex.[44]

It is enlightening to compare these findings to those for other binuclear iron complexes linked by covalent bonds at the metal cores (group three in the Introduction). In this study, no evidence inferring metal–metal interaction was obtained. Yet iron porphyrins with single-atom bridging moieties demonstrate significant ligand-mediated metal–metal interactions. Mixed-valence complexes have been isolated and studied in detail.[12–14] The bridging-ligand–iron-core interaction in the single-atom-bridged dimers differs from that of the binuclear complexes reported herein in two ways. First, the Fe atom is displaced from the porphyrin core toward the bridging atom from 26 to 50 pm.[14c] Second, the Fe atom–bridging-ligand interactions are not dynamic. We have

shown that cobalt porphyrins possessing a steric superstructure on one side of the porphyrin demonstrated significantly diminished axial ligand dynamics.[45] Perhaps multiatom-bridged binuclear complexes can be isolated by using the Fe derivatives of sterically encumbered porphyrins. These complexes would presumably possess pentacoordinate Fe centers displaced from the porphyrin plane toward the bridging moiety. This displacement would maximize the metal–ligand π-orbital overlap (a necessary and sufficient condition for intervalence transfer[46]) and minimize the coulostatic repulsion between the porphyrin and the exo-bidentate bridging moiety. The synthesis of such molecules is currently under way in anticipation that from these multiatom-bridged complexes mixed-valence materials can be prepared.

Registry No. py, 110-86-1; 4-pic, 108-89-4; PYAN, 4916-57-8; PYEN, 1135-32-6; BIPY, 87378-14-1; DABCO, 280-57-9; PYZ, 290-37-9; (TPP)FeCS, 67583-11-3; (TPP)FeCS(py), 67670-43-3; (TPP)-FeCS(4-pic), 92054-38-1; (TPP)FeCS(PYAN), 116349-62-3; (TPP)-FeCS(PYEN), 116349-63-4; (TPP)FeCS(BIPY), 116349-64-5; (TPP)-FeCS(DABCO), 116349-65-6; (TPP)FeCS(PYZ), 116349-66-7; [(TPP)FeCS]$_2$(PYAN), 116349-67-8; [(TPP)FeCS]$_2$(PYEN), 116349-68-9; [(TPP)FeCS]$_2$(BIPY), 116349-69-0; [(TPP)FeCS]$_2$(DABCO), 116349-70-3; [(TPP)FeCS]$_2$(PYZ), 116349-71-4; {[(TPP)FeCS]$_2$-(PYZ)}$^{2-}$, 116349-73-6; {[(TPP)FeCS]$_2$(BIPY)}$^{2-}$, 116349-74-7; {[(TPP)FeCS]$_2$(PYAN)}$^{2-}$, 116349-72-5; {[(TPP)FeCS]$_2$(PYEN)}$^{2-}$, 116374-40-4; {[(TPP)FeCS]$_2$(DABCO)}$^{2-}$, 116349-75-8; [(TPP)FeCS-(PYZ)]$^-$, 116349-95-2; [(TPP)FeCS(BIPY)]$^-$, 116349-96-3; [(TPP)-FeCS(PYAN)]$^-$, 116349-76-9; [(TPP)FeCS(PYEN)]$^-$, 116349-77-0; [(TPP)FeCS(DABCO)]$^-$, 116349-78-1; {[(TPP)FeCS]$_2$(PYZ)}$^{2+}$, 116349-79-2; {[(TPP)FeCS]$_2$(BIPY)}$^{2+}$, 116349-80-5; {[(TPP)FeCS]$_2$-(PYAN)}$^{2+}$, 116349-81-6; {[(TPP)FeCS]$_2$(PYEN)}$^{2+}$, 116349-82-7; [(TPP)FeCS(PYZ)]$^+$, 116349-83-8; [(TPP)FeCS(BIPY)]$^+$, 116349-84-9; [(TPP)FeCS(PYAN)]$^+$, 116349-85-0; [(TPP)FeCS(PYEN)]$^+$, 116349-86-1; {[(TPP)FeCS]$_2$(PYZ)}$^{4+}$, 116349-87-2; {[(TPP)FeCS]$_2$-(BIPY)}$^{4+}$, 116349-88-3; {[(TPP)FeCS]$_2$(PYAN)}$^{4+}$, 116349-89-4; {[(TPP)FeCS]$_2$(PYEN)}$^{4+}$, 116349-90-7; [(TPP)FeCS(PYZ)]$^{2+}$, 116349-91-8; [(TPP)FeCS(BIPY)]$^{2+}$, 116349-92-9; [(TPP)FeCS-(PYAN)]$^{2+}$, 116349-93-0; [(TPP)FeCS(PYEN)]$^{2+}$, 116349-94-1; tetra-n-butylammonium perchlorate, 1923-70-2.

(44) Oxidation of the electrochemically generated thioformyl Fe(II) porphyrin anion occurred at $E_p = -0.50$ V. In the presence of L or L-L, oxidation of the thioformyl Fe(II) porphyrin occurred at $E_p = -0.48$ V (at 200 mV s^{-1}). This potential insensitivity to the presence and/or identity of L or L-L suggests either that the thioformyl Fe(II) porphyrin anion contains a five-coordinate Fe center or that the electron-transfer reaction is porphyrin-ring-centered.

(45) Bottomley, L. A.; Gorce, J.-N.; Davis, W. M. *J. Electroanal. Chem. Interfacial Electrochem.* **1986**, *202*, 111.
(46) Richardson, D. E.; Taube, H. *Coord. Chem. Rev.* **1984**, *60*, 107 and references therein.